

LCNC in the paranasal sinus is a rare presentation. The first case in the sinonasal region was described in 1982. Although the anatomical characteristics of the sinonasal region predispose to nonspecific clinical features initially, rapid growth can alter the presentation dramatically, with mass-effect related symptoms, as in the case presented here<sup>(9)</sup>. Imaging studies are essential for diagnostic and staging. On CT, a neuroendocrine carcinoma usually presents as a heterogeneous soft-tissue mass without calcifications and with strong contrast enhancement<sup>(10,11)</sup>. In one case series of patients with primary neuroendocrine carcinoma<sup>(11)</sup>, MRI showed hypointensity on T1WI in 91% of the cases and hyperintensity on T2WI in 83%, with intense contrast enhancement in all cases. Our case differs only in terms of the T2WI isointensity observed, which we believe reflects the high cellularity and low free-water content of the tumor. These characteristics are nonspecific, and it is not possible to differentiate neuroendocrine carcinoma from other more common etiologies, such as squamous cell carcinoma and lymphoma, on the basis of imaging findings alone<sup>(12)</sup>.

Staging follows the tumor-node-metastasis criteria, CT and MRI being complementary, due the better soft-tissue resolution of the latter, which allows better evaluation of skull base invasion. The evaluation of metastases should not rely on functional studies alone, because LCNC metastasis may lack octreotide/somatostatin uptake<sup>(13)</sup>. Zhou et al. found that 81% of neuroendocrine carcinomas were at least stage T3 on presentation<sup>(11)</sup>. The rapid progression and advanced stage of the tumor at diagnosis denotes the malignant behavior of LCNC, which limits the proportion of patients who are candidates for surgery and, consequently, reduces survival.

#### REFERENCES

- Alves MLD, Gabarra MHC. Comparison of power Doppler and thermography for the selection of thyroid nodules in which fine-needle aspiration biopsy is indicated. *Radiol Bras.* 2016;49:311–5.
- Reis I, Aguiar A, Alzamora C, et al. Locally advanced hypopharyngeal squamous cell carcinoma: single-institution outcomes in a cohort of patients curatively treated either with or without larynx preservation. *Radiol Bras.* 2016;49:21–5.
- Ribeiro BNF, Marchiori E. Rosai-Dorfman disease affecting the nasal cavities and paranasal sinuses. *Radiol Bras.* 2016;49:275–6.
- Cunha BMR, Martin MF, Indiani JMC, et al. Giant cell tumor of the frontal sinus: a typical finding in an unlikely location. *Radiol Bras.* 2017;50:414–5.
- Moreira MCS, Santos AC, Cintra MB. Perineural spread of malignant head and neck tumors: review of the literature and analysis of cases treated at a teaching hospital. *Radiol Bras.* 2017;50:323–7.
- Ferlito A, Strojan P, Lewis JS Jr, et al. Large cell neuroendocrine carcinoma of the head and neck: a distinct clinicopathologic entity. *Eur Arch Otorhinolaryngol.* 2014;271:2093–5.
- Dogan M, Yalcin B, Ozdemir NY, et al. Retrospective analysis of seventy-one patients with neuroendocrine tumor and review of the literature. *Med Oncol.* 2012;29:2021–6.
- Moran CA, Suster S. Neuroendocrine carcinomas (carcinoid, atypical carcinoid, small cell carcinoma, and large cell neuroendocrine carcinoma): current concepts. *Hematol Oncol Clin North Am.* 2007;21:395–407, vii.
- Bell D, Hanna EY, Weber RS, et al. Neuroendocrine neoplasms of the sinonasal region. *Head Neck.* 2016;38(Suppl 1):E2259–66.
- Sowerby LJ, Matthews TW, Khalil M, et al. Primary large cell neuroendocrine carcinoma of the submandibular gland: unique presentation and surprising treatment response. *J Otolaryngol.* 2007;36:E65–9.
- Zhou C, Duan X, Liao D, et al. CT and MR findings in 16 cases of primary neuroendocrine carcinoma in the otolaryngeal region. *Clin Imaging.* 2015;39:194–9.
- Kanamalla US, Kesava PP, McGuff HS. Imaging of nonlaryngeal neuroendocrine carcinoma. *AJNR Am J Neuroradiol.* 2000;21:775–8.
- Subedi N, Prestwich R, Chowdhury F, et al. Neuroendocrine tumours of the head and neck: anatomical, functional and molecular imaging and contemporary management. *Cancer Imaging.* 2013;13:407–22.

**Helder Groenwold Campos<sup>1</sup>, Albina Messias Altemani<sup>1</sup>, João Altemani<sup>1</sup>, Davi Ferreira Soares<sup>1</sup>, Fabiano Reis<sup>1</sup>**

1. Universidade Estadual de Campinas (Unicamp), Campinas, SP, Brazil. Mailing address: Dr. Helder Groenwold Campos. Universidade Estadual de Campinas – Radiologia. Rua Tessália Vieira de Camargo, 126, Cidade Universitária. Campinas, SP, Brazil, 13083-887. E-mail: heldergcampos@gmail.com.

<http://dx.doi.org/10.1590/0100-3984.2016.0184>



This is an open-access article distributed under the terms of the Creative Commons Attribution License.

#### Differential diagnosis of pathological intracranial calcifications in patients with microcephaly related to congenital Zika virus infection

Dear Editor,

Congenital central nervous system infections are accompanied by pathological intracranial calcifications, and cerebral organogenesis malformations are common in viral infections, particularly when they occur in the first trimester of gestation<sup>(1–5)</sup>. Intracranial calcifications with brain malformations have been reported in cytomegalovirus infection, congenital rubella, and, more recently, in Zika virus infection<sup>(1,2,4,5)</sup>. In cases of congenital toxoplasmosis, calcifications are seen in 50–80% of cases and hydrocephalus is a common finding, although defects in organogenesis induced by nonviral etiologic agents are rare<sup>(3,4)</sup>.

In the neonatal period, the diagnosis of congenital cytomegalovirus infection can be simple in a child presenting with fever, jaundice, hepatosplenomegaly, anemia, thrombocytopenia, and retinopathy. In cases of Zika virus infection, the central clinical aspect is microcephaly<sup>(2,3,6,7)</sup>. In congenital cytomegalovirus infection, the characteristic presentation is brain calcifications. Those calcifications are often periventricular, in the ependymal or subependymal region, appearing as points or lines or, in some cases, delineating the ventricles. The calcification foci,

which can occur in the basal ganglia, white matter, or cortex, are often asymmetric<sup>(1–5)</sup>.

Although congenital rubella is exceptionally rare in Brazil, some cases have been reported. The radiological findings are similar to those of cytomegalovirus infection. White matter anomalies and periventricular calcifications are often present, as are calcifications in the basal ganglia<sup>(4)</sup>. Unlike other congenital viral infectious processes associated with encephalic malformations, in which the distribution is typically periventricular, the Zika virus appears to produce subcortical calcifications (Figure 1).

The association among intracranial calcifications, congenital infections, and central nervous system malformations is broad and requires the observance of some aspects. Congenital microcephaly can be divided into two main categories: primary and secondary. Some patients with primary congenital microcephaly have been described as having congenitally small but architecturally normal brains, which does not occur in cases of microcephaly associated with diverticulum and cleavage malformations such as holoprosencephaly or cerebral cortical defects such as lissencephaly, usually associated with nonprogressive mental retardation of a presumed genetic cause. In contrast, in cases of microcephaly acquired as a result of brain damage, such as those associated with hypoxic-ischemic injury, congenital central

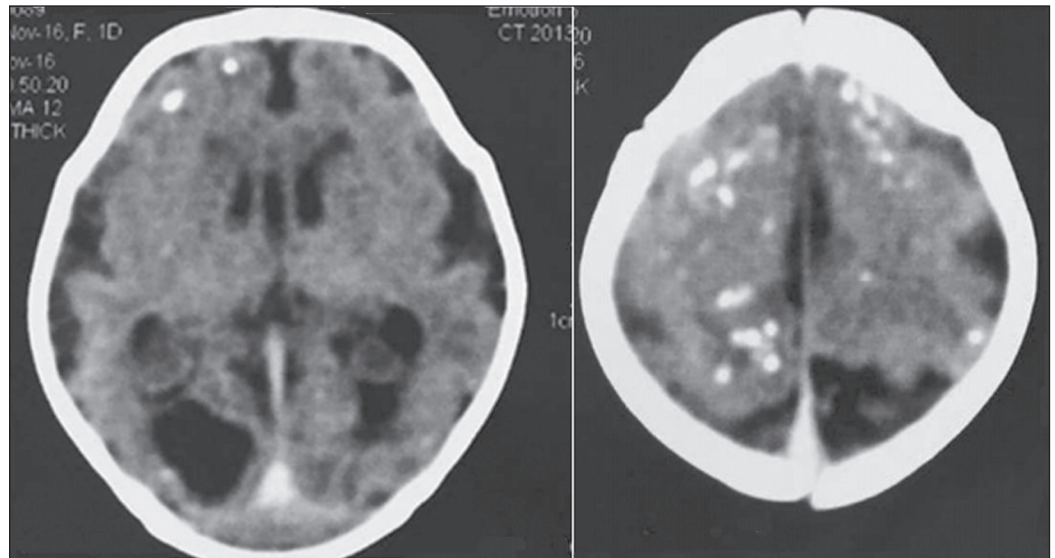


**Figure 1.** Non-contrast-enhanced computed tomography of the brain in a one-day-old neonate with lesions attributed to Zika virus infection, showing subcortical pathological intracranial calcifications and microcephaly with a compromised aspect of the cerebral sulci, malformation of the opercula, marked reduction in the cerebral white matter volume, and ventricular dilation.

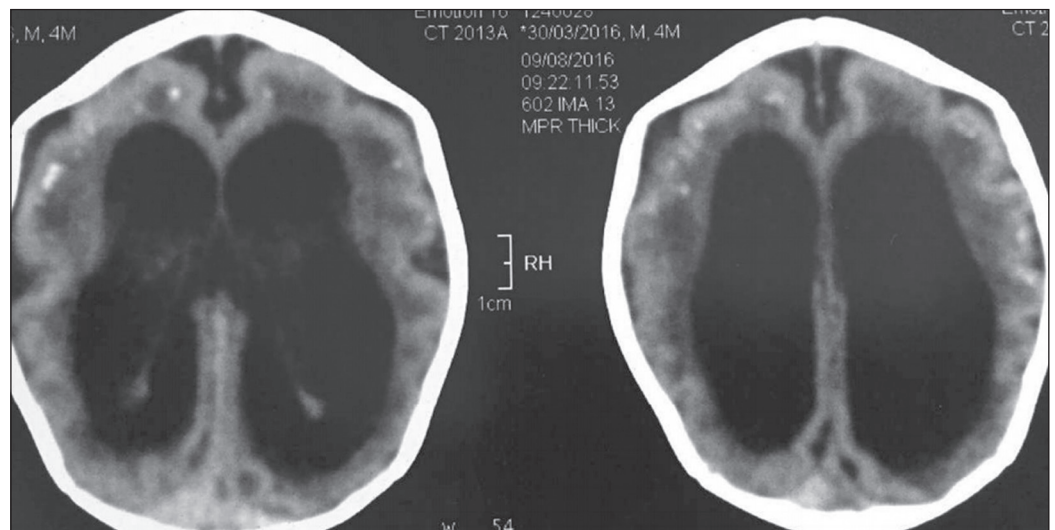


**Figure 2.** Non-contrast-enhanced computed tomography of the brain in a four-month-old child with lesions attributed to Zika virus infection, showing pathological subcortical intracranial calcifications, microcephaly, and ventricular dilatation, with simplification of the cerebral convolutions.

nervous system infection, or metabolic disease, the head size can initially be normal but can decrease as a result of the brain injury. However, in cases of Zika virus infection, microcephaly and brain calcifications, with simplification of the cerebral convolutions, are present on the first day of life (Figure 2).

The causes of pathological intracranial calcifications in children are diverse. Nevertheless, the combination of microcephaly and defects of cerebral organogenesis, especially those related to impairment of neuronal migration, is a strong indication of congenital central nervous system infection with a viral agent, and subcortical predominance of calcifications should prompt the radiologist to consider the hypothesis of Zika virus infection.

**REFERENCES**

1. Teissier N, Fallet-Bianco C, Delezoide AL, et al. Cytomegalovirus-induced brain malformations in fetuses. *J Neuropathol Exp Neurol.* 2014;73:143–58.
2. Soares de Oliveira-Szejnfeld P, Levine D, Melo ASO, et al. Congenital

brain abnormalities and Zika virus: what the radiologist can expect to see prenatally and postnatally. *Radiology.* 2016;281:203–18.

3. Adachi Y, Poduri A, Kawaguchi A, et al. Congenital microcephaly with a simplified gyral pattern: associated findings and their significance. *AJNR Am J Neuroradiol.* 2011;32:1123–9.
4. Livingston JH, Stivaros S, Warren D, et al. Intracranial calcification in childhood: a review of aetiologies and recognizable phenotypes. *Dev Med Child Neurol.* 2014;56:612–26.
5. Fink KR, Thapa MM, Ishak GE, et al. Neuroimaging of pediatric central nervous system cytomegalovirus infection. *Radiographics.* 2010;30:1779–96.
6. Niemeyer B, Muniz BC, Gasparetto EL, et al. Congenital Zika syndrome and neuroimaging findings: what do we know so far? *Radiol Bras.* 2017;50:314–22.
7. Rafful P, Souza AS, Tovar-Moll F. The emerging radiological features of Zika virus infection. *Radiol Bras.* 2017;50(6):vii–viii.

**Alexandre Ferreira da Silva<sup>1</sup>**

1. Ecotomo S/S Ltda., Belém, PA, Brazil. Mailing address: Dr. Alexandre Ferreira da Silva. Ecotomo S/S Ltda. Rua Bernal do Couto, 93, ap. 1202, Umarizal. Belém, PA, Brazil, 66055-080. E-mail: alexandreecotomo@oi.com.br.

<http://dx.doi.org/10.1590/0100-3984.2016.0219>

 This is an open-access article distributed under the terms of the Creative Commons Attribution License.